Int. J. Plant Sci. 178(8):629–638. 2017.

1058-5893/2017/17808-0005$15.00 DOI: 10.1086/693857

MICROSCOPIC CHARACTERIZATION OF A TRANSPOSON-INDUCED MALE-STERILE, FEMALE-STERILE MUTANT IN *GLYCINE MAX* L.

Katherine A. Thilges,[1,*,†] Mark A. Chamberlin,[‡] Marc C. Albertsen,[†] and Harry T. Horner[*]

*Department of Genetics, Development, and Cell Biology and Microscopy and NanoImaging Facility, Iowa State University, Ames, Iowa 50011, USA; †DuPont Pioneer, 7300 Northwest 62nd Avenue, Johnston, Iowa 50131, USA; and ‡7019 Sunset Terrace, Windsor Heights, Iowa 50324, USA

Editor: John L. Bowman

Premise of research. A male-sterile, female-sterile mutant was discovered in a *w4*-m mutable line of *Glycine max* L. The mechanism of its sterility was not well understood. Therefore, different cytological and microscopic techniques were undertaken to better understand the process of mutant phenotype development. Molecular research indicated that *mer3* was responsible for the sterility.

Methodology. Macro images were collected of whole plants, flowers, anthers, pods, and ovules. Chromosome spreads from anthers at various meiotic stages were examined. Confocal scanning laser microscopy using optical sectioning was utilized on whole anthers and ovules at various developmental stages. Whole mature anthers and isolated pollen images were collected and studied with SEM.

Pivotal results. In observations of the mutant, male cell development was found to begin normally and then digresses at metaphase I of meiosis, when abnormal segregation of chromosomes with reduced bivalent formation was observed. It was the abnormal formation of univalents and bivalents that led to male sterility. On the female side, the progression of development was arrested in the megagametophyte stage likely because of abnormal meiosis, leading to ovule abortion and female sterility.

Conclusions. The *G. max* male-sterile, female-sterile mutant was shown to have the same phenotype of *mer3* sterility already shown in *Arabidopsis*, rice, yeast, and some animal systems.

Keywords: female sterility (FS), *Glycine max*, male sterility (MS), *mer3*, soybean, transposon.

Introduction

The *w4*-mutable line (T322) of soybean was found in an F_7 generation of a cross between two breeding lines of Asgrow Seed (Palmer et al. 1989). In these plants, flowers were white, purple, or variegated in color. Analysis revealed that the floral traits were conditioned by an unstable recessive allele, *w4*-m, caused by insertion of a CACTA-type active transposable element in the *DFR2* gene located in the *w4* locus. *DFR2* encodes dihydroflavonol-4-reductase 2, which is involved in anthocyanin biosynthesis (Xu et al. 2010). Mutable plants of the *w4*-mutable line are homozygous for mutable alleles at the *W4* locus. Wild-type progeny (germinal revertants) are produced by mutable plants when the *w4*-m allele reverts to wild type (Palmer et al. 1989). The *w4*-mutable line is wild type for the anthocyanin pigment. This unstable allele, *w4*-m, reverts at high frequency to the wild-type *W4* allele (Palmer et al. 1989).

Xu et al. (2010) confirmed that when the transposon *Tgm9* was excised from *DFR2* intron II, an anthocyanin locus, the *DFR2* expressed and gave a purple flower phenotype. *Tgm9* is a low-copy-number element like most CACTA elements. These CACTA elements excise at a high frequency (Xu et al. 2010). It is the excision of *Tgm9* from *DFR2* into *mer3* that causes the mutation in the *w4* lines.

A male-sterile, female-sterile (MSFS) mutant from a germinal revertant of the *w4*-m line bearing purple flowers was found at Iowa State University (Raval et al. 2013). The locus was mapped to molecular linkage group J (chromosome 16) through bulked segregant analysis. A 62-kb region was found, and fine mapping indicated that the region contained only five genes. One of the genes in that region, identified as *Glyma.16G072300*, encodes a helicase gene (Raval et al. 2013). A rice homolog of this helicase gene has been shown to control crossing over and a sterility phenotype (Wang et al. 2009). *Glyma.16G072300* is then most likely the gene regulating the male and female sterility phenotype in the mutant soybean (Raval et al. 2013). DNA blot analysis was done for individuals that were segregating for *Tgm9*. A perfect association was shown between sterility in the plant and the presence of the transposon *Tgm9* in the sterility locus (Raval et al. 2013).

Molecular analysis of two independent revertant plants showed that excision of *Tgm9* from *Glyma.16G072300* had resulted in the fertile branches, confirming that mutation in the helicase

[1] Author for correspondence; e-mail: katherine.thilges@pioneer.com.

Manuscript received April 2017; revised manuscript received June 2017; electronically published August 29, 2017.

Table 1

Genotyping Results from *w4*-m Lines in Soybean

Line	Wild type (%)	Heterozygous (%)	Mutant (%)
A05-221-1	30 (27.77)	46 (42.59)	32 (29.62)
A05-221-3	36 (34.61)	48 (46.15)	20 (19.23)
A05-221-4	106 (99.06)	1 (.93)	0 (.00)
A05-221-5	28 (25.22)	51 (45.94)	32 (28.82)

Note. Each line represents a different line of the *w4*-m soybean line containing the *Tgm9* transposon.

gene causes male and female sterility (Raval et al. 2013). Phylogenetic analysis placed the gene in a clade with the *Arabidopsis* and rice MER3 proteins and suggested that it is the only *MER3*-like gene in soybean (Baumbach et al. 2016). This gene is expressed in flower buds, trifoliolate leaves, and stems; however, there was no transcript detected in cotyledons or roots (Baumbach et al. 2016).

The purposes of this study were threefold: to conduct a microscopic study to determine phenotypes of the male-sterile and female-sterile mutant caused by insertion of *Tgm9* in a *MER3*-like gene recently identified by Baumbach et al. (2016), to identify any abnormalities during meiosis that were *MER3*-like, and to follow the development of anthers and ovules to pinpoint when sterility occurs and what tissues may be affected in the mutant. These results were compared with the molecular study (Baumbach et al. 2016) to understand the fertility mechanisms in soybean.

Material and Methods

Plants

The *w4*-mutable line of soybean is an unstable mutation for purple flower color at the *W4* locus. It was found in the F_7 generation of a cross between breeding line X1878 (Amsoy 17 X AG52109) and X2717 (Corsoy X Essex; Weigelt et al. 1990). From this progeny of the *w4*-m line, an MSFS mutant was identified, ASR-10-181 (A05-221, segregating background number; Baumbach et al. 2016). This *w4*-m mutant (MT) line and a comparable wild-type (WT) line (Minsoy) were used in this study.

Growth of Plants

All plants (seven rounds of plantings) were grown under identical greenhouse conditions at the DuPont Pioneer Soy Research Facility (Johnston, IA). The lighting schedule started at 16 h of light for 25 d and then decreased in the following sequence: 15.5 h for 3 d; 15 h for 3 d; 14.5 h for 3 d; 14 h for 25 d; 13.5 h for 3 d; 13 h for 3 d; 12.5 h for 3 d; and 12 h for approximately 25 d, or until complete dry down and then harvest. Throughout the growing cycle the daytime temperature was set at 81°–83°F, and the nighttime temperature was 71°–73°F. Seeds were initially started in flats with a standard soil mix and then were transplanted into pots with a Fafard 3B growing mix (http://www.sungro.com).

Greenhouse Whole Plants and Flowers

Whole WT and MT plants were imaged in the greenhouse with a Nikon D70 digital single-lens reflex camera starting at 4 wk after germination and were imaged once a week for 4 wk to monitor for any vegetative differences between WT and MT plants. Whole flowers and buds were collected at different stages and imaged fresh with a Zeiss Axio Zoom V16 (http://www.zeiss.com) and Leica M165FC with the Leica DFC310 FX camera (http://www.leica-microsystems.com) stereomicroscopes.

Sampling and DNA Extraction

Plants from all plantings were sampled at 2 wk after germination on dry ice with two leaf punches for each plant. Samples were stored at −80°C until DNA extraction. DNA extraction was done using the DNeasy Plant Mini Kit from Qiagen (http://www.qiagen.com).

DNA Analysis to Identify WT and MT Plants

Polymerase chain reaction was set up using the Rev1, TransR1, and TransR2 primers (Baumbach et al. 2016). The reaction was completed using a Bio-Rad C100 Thermal Cycler, and samples were run on a 1.5% agarose gel. The gels were imaged on an AlphaImager Mini (http://www.proteinsimple.com).

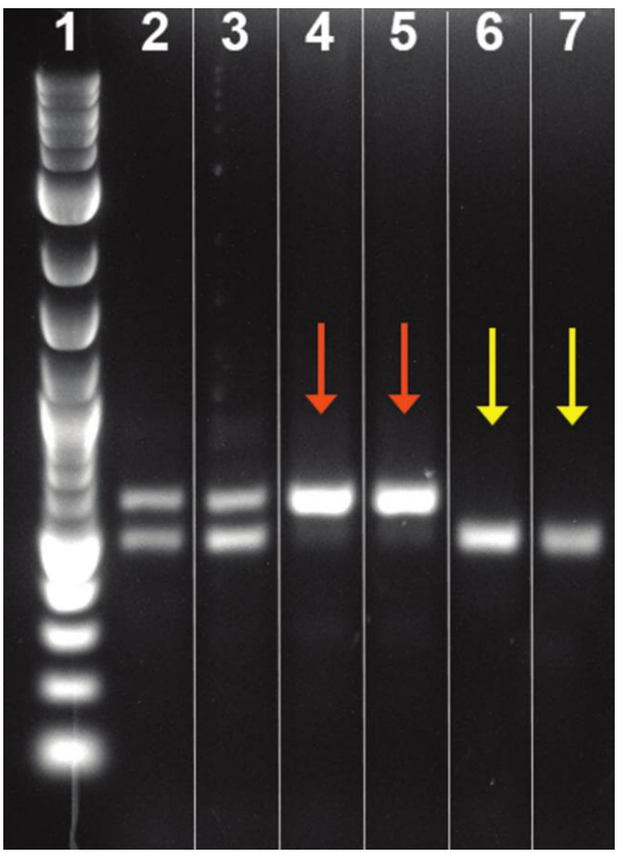

Fig. 1 Polymerase chain reaction results from genotyping of *w4*-m soybean lines. Lane 1 contains log20 DNA ladder. Lanes 2 and 3 show banding pattern of a heterozygous line with the 491- and 601-bp bands. Lanes 4 and 5 show banding pattern of *Tgm9* male-sterile, female-sterile mutant with a 601-bp fragment (orange arrows). Lanes 6 and 7 show wild-type banding pattern with a 491-bp band (yellow arrows).

Table 2

Number of Wild-Type and Mutant Plants Collected and Observed for Different Microscopic Techniques

		Observed			
	Collected	Chromosome spreads	Acetocarmine staining	CSLM	SEM
Mutant	84	15	12	32	6
Wild type	26	8	8	10	2

Note. Each plant was collected at multiple times during flowering to obtain developmental stages for observation. CSLM = confocal scanning laser microscope.

Chromosome Spreads

Young anthers of both WT and MT plants were fixed in 3:1 ethanol (EtOH):glacial acetic acid solution. Samples were then processed according to Ross et al. (1996). The sections were mounted and stained with Vectashield with DAPI (http://www.vectorlabs.com) and then imaged with the Leica DMRXA fluorescence microscope using a DAPI filter with 360–370-nm excitation and 435–485-nm emission (http://www.chroma.com) and a Hamamatsu Orca Flash 4.0LT camera (http://www.hamamastu.com).

Acetocarmine Staining

Anthers were collected at different developmental stages and fixed in 3:1 EtOH:glacial acetic acid, and the fixative solution was changed until it was clear. The anthers were dissected to release the male cells into 2% acetocarmine and imaged using the Leica DMRXA with a Leica DFC450 camera.

Alexander Staining

Anthers were collected and fixed in 3:1 EtOH:glacial acetic acid, and the fixative solution was changed until it was clear. The anthers were then dissected and stained according to Peterson et al. (2010). The pollen was then imaged on the Leica DMRXA with a Leica DFC450 camera.

Fixation and Clearing for Anther and Ovule Analyses Using a Confocal Scanning Laser Microscope (CSLM)

Whole flowers were collected at different developmental stages and fixed in 2% paraformaldehyde:4% glutaraldehyde in phosphate buffered saline (PBS; pH 7.2) and vacuum infiltrated at 10 psi to speed up the penetration of fixative. Samples were rinsed in PBS and dehydrated in a graded EtOH series. On reaching 100% EtOH, the samples were cleared in benzyl alcohol:benzyl benzoate (BABB) using the procedure from Bioengineering Confocal and Multiphoton Imaging Core Facility (2000; http://www.seas.upenn.edu/~confocal/Clearing_agents.html#babb). Samples were mounted on slides in BABB and imaged using the Leica TCS SPE CSLM with 405-, 488-, and 561-nm laser lines.

SEM

Mature WT and MT anthers and gynoecia at pollen dehiscence were fixed in FAA (formalin, acetic acid, EtOH; Ruzin 1999) and dehydrated in a graded EtOH series to pure EtOH. At this point the samples were critical-point dried (http://www.dentonvacuum.com). Some of the anthers were teased open, mounted on aluminum stubs with double-sided sticky tabs, and surrounded with silver paint. The samples were then sputter-coated with palladium gold (60:40) and observed using a JEOL 5800 SEM (http://www.jeolusa.com) at 10 kV.

Results

Various microscopic techniques and three different chemical fixation procedures were used to provide information on the developmental sequence of events that occur during WT and MT anther and ovule development. All three fixation procedures provided comparable anatomical results. Once the WT soybean developmental patterns for anthers and ovules were established, they were compared with the same developmental patterns in the MT plants. A total of 430 plants were grown and genotyped (table 1; fig. 1). Flowers were collected from MT and WT plants at various stages of development for different microscopic procedures (table 2).

Whole Plant Images

Whole plant images were taken beginning 4 wk after planting and then weekly until 8 wk after planting. No differences were discerned between the WT and the MT vegetative plants (fig. 2*A*, 2*B*). The only visible difference at the time of flowering was the lack of mature pod formation on the MT plants (fig. 2*C* [WT], 2*D* [MT]).

Inspection of the early pods (gynoecia) on the WT (fig. 2*E*) and MT (fig. 2*F*) plants revealed that in the MT pods, the ovules (fig. 2*J*) were arrested at an early stage of development in contrast to WT ovules (fig. 2*I*). Development of the flowers progressed normally for both the WT (fig. 2*L*) and the MT (fig. 2*K*) plants, and visible shed pollen (or arrested late microspores/pollen) was observed from both the WT (fig. 2*G*) and the MT (fig. 2*H*) anthers.

Acetocarmine Staining

Acetocarmine staining was carried out on the WT (fig. 3*A*, 3*C*, 3*E*, 3*G*, 3*I*) and MT (fig. 3*B*, 3*D*, 3*F*, 3*H*, 3*J*) male cells from the premeiotic sporogenesis mass stage to the mature pollen stage. The MT male cells progressed normally (fig. 3*B*, 3*D*, 3*F*) until the tetrad stage, when a mixture of normal-appearing tetrads and abnormal-appearing triads and pentads (fig. 3*H*) were observed; some of the latter with mini-microspores were evident. Counts were done to quantify the number of WT and MT male cells that appeared at the tetrad stage (table 3). On release from their callose the MT microspores displayed various sizes, with some that were collapsed. By the pollen stage this condition of variable size in MT pollen was clearly evident (fig. 3*J*).

Alexander Staining for Pollen Viability

Both WT (fig. 4*A*) and MT (fig. 4*B*–4*D*) showed cytoplasmic staining at their respective pollen stages. However, the MT pollen displayed various sizes and shapes and often with plasmolyzed cytoplasm. As mentioned later, none of the MT pollen germinated when released from the anthers onto the stigmas,

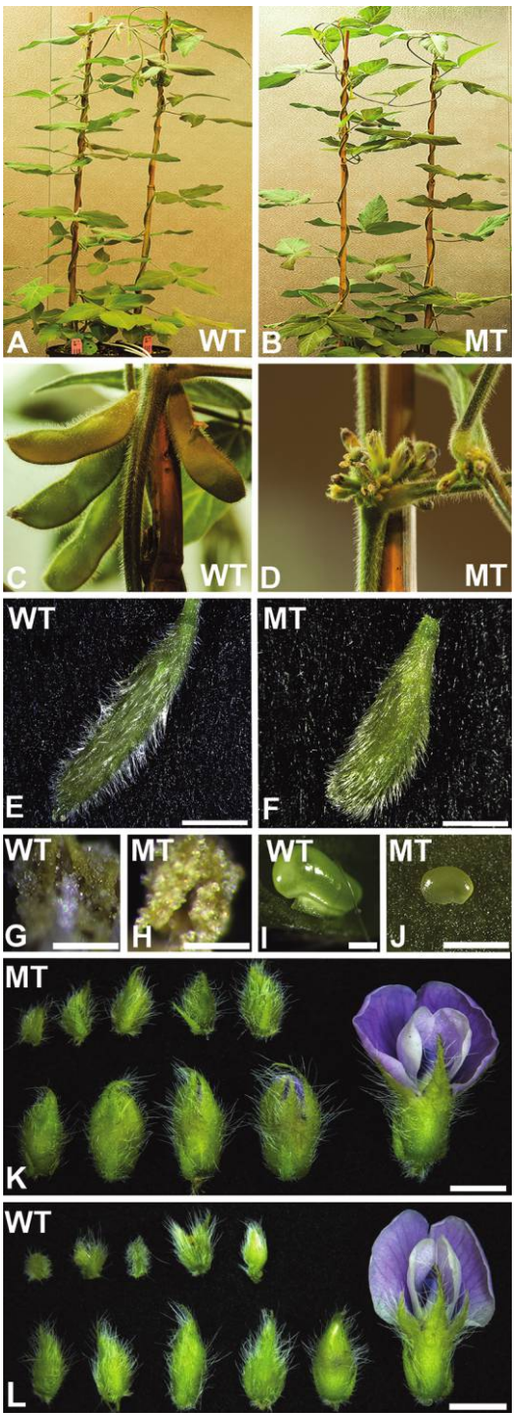

Fig. 2 Whole plant and flower images of wild-type (WT) and mutant (MT) soybean plants. *A*, Whole WT plant 5 wk after planting. *B*, Whole MT plant 5 wk after planting. *C*, Close-up of pods on a WT plant 6 wk after planting. *D*, Lack of pod formation on an MT plant 6 wk after planting. *E*, Early pod from a WT plant. *F*, Early pod on an MT plant. *G*, WT anther showing dehisced pollen. *H*, MT anther showing dehisced pollen. *I*, *J*, WT ovule (*I*) in comparison to an MT ovule (*J*), where development is arrested at a young stage. *K*, *L*, Bud to flower progression of an MT plant (*K*); appears identical to a WT plant (*L*). Scale bars = 5 mm (*E*, *F*), 200 μm (*G*, *H*), 500 μm (*I*, *J*), 2 mm (*K*, *L*).

nor were any viable pods formed on the MT plants when self-pollinated or hand-pollinated with WT Minsoy plants.

Chromosome Spreads

Chromosome spreads of fixed anthers revealed no visible differences between WT (fig. 5*A*–5*D*) and MT (fig. 5*E*–5*H*) meiotic male cells from early prophase until metaphase I (fig. 5*I*–5*N*). At this stage, both univalents and bivalents are clearly

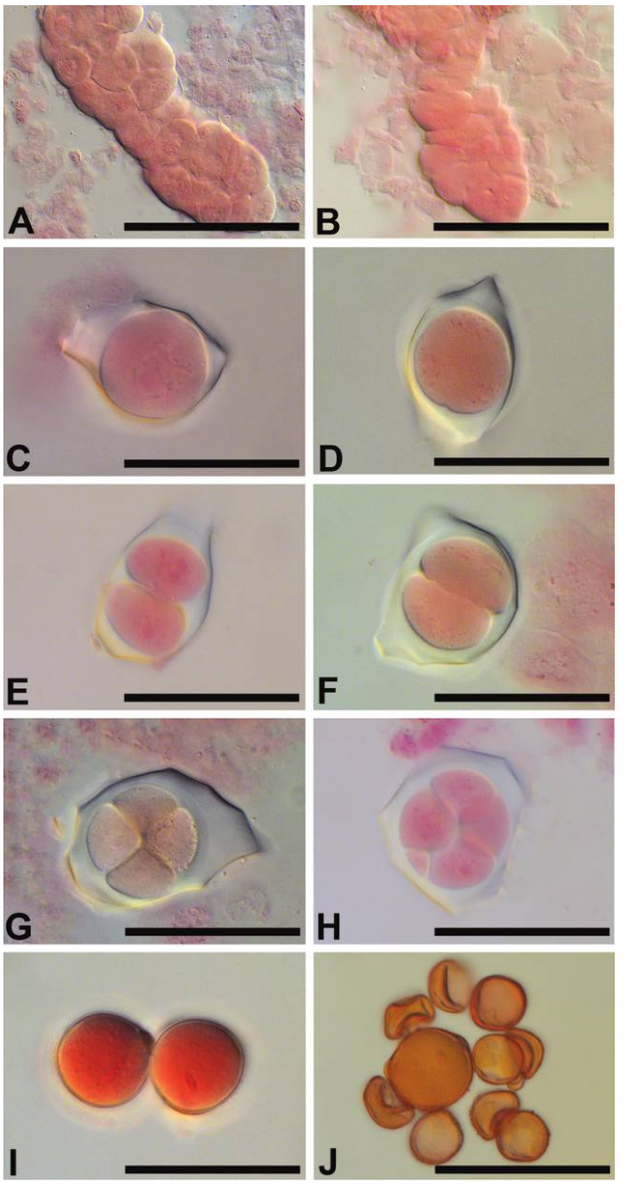

Fig. 3 Acetocarmine staining of wild-type (WT; *A*, *C*, *E*, *G*, *I*) and mutant (MT; *B*, *D*, *F*, *H*, *J*) male cell development. *A*, WT = sporogenous mass. *C*, WT = meiocyte. *E*, WT = dyad. *G*, WT = tetrad. *I*, WT = pollen. *B*, MT = sporogenous mass. *D*, MT = meiocyte. *F*, MT = dyad. *H*, MT = pentad. Callose walls surround male cells in *C*–*H*. *J*, MT = variable-sized and collapsed pollen. Scale bars = 50 μm (*A*, *B*), 20 μm (*C*–*J*).

Table 3

Wild-Type and Mutant Male Cell Tetrad Stage Counts from Acetocarmine Staining

	Tetrads	Uneven Tetrads	Triads	Pentads
Wild type	50	0	0	0
Mutant	7	18	11	14

Note. These counts were done across multiple anthers from multiple plants.

visible in the MT (fig. 5*L*, 5*M*). MT chromosomes displayed significantly fewer bivalents (3–9; in fig. 5*I* [WT] and 5*L* [MT], bivalents are labeled with asterisks) and unpaired homologous chromosomes than the normal complement of WT bivalents that is 20 (fig. 5*I*, 5*J*). This reduction in bivalents was noted across numerous samples. Ovule squashes to observe chromosomes were not attempted, but their early abnormal development as observed using CSLM strongly suggested that the same abnormalities of chromosome pairing and synapsis occurred during female meiosis in the MT ovules.

CSLM of Cleared WT and MT Anthers and Ovules

Overfixation of glutaraldehyde induced differential autofluorescence of the components of the internal cells and tissues of the anthers and ovules. This fluorescence made cell types and stages of development easily distinguishable in optical sections and as clear as the more tedious method of physical sectioning.

WT and MT Anther Development

WT pollen development began with the differentiation of premeiotic sporogenous mass within the anther (fig. 6*A*), followed by continued differentiation of the meiocytes and the formation of a thick callose wall that surrounds each meiocyte (fig. 6*B*). The meiocytes underwent two meiotic divisions to produce dyads and then tetrads of haploid microspores (fig. 6*C*). This was followed by breakdown of the callose and release of the young microspores (fig. 6*D*). As the microspores progressed into midmicrospore stage, their small vacuoles began to coalesce. The union of these small vacuoles as well as thickening of the surrounding exine wall signaled their progression to the late microspore stage, when mitosis gave rise to binucleate and vacuole pollen (fig. 6*E*). The continuing development of the exine wall and the accumulation of storage reserves completed the progression into midpollen and finally mature pollen, where the generative nucleus then divided to form two sperm (fig. 6*F*).

The MT male cells, similar to the WT male cells, developed normally (fig. 6*G*, 6*H*) until meiosis, when (cytologically) chromosome pairing abnormalities occurred that translated into malformed, different-sized tetrads as well as triads and pentads (fig. 6*I*). These abnormalities accumulated in the microspore stage after release from the tetrads, where the released microspores (fig. 6*J*) showed abnormal sizes ranging from relatively small to large when compared with uniform-sized WT microspores (fig. 6*D*). Even though MT microspore development continued, the highly vacuolated microspores of different sizes eventually collapsed or were misshapen and did not develop into viable pollen (fig. 6*K*, 6*L*).

WT and MT Ovule Development

WT ovule primordium was comprised of several hypodermal primordial cells (fig. 7*A*) where one cell enlarged (the archesporial cell; fig. 7*B*) that became the functional megasporocyte or megaspore mother cell. This cell underwent meiosis I to produce a dyad (fig. 7*C*) and then meiosis II to produce a linear tetrad of megaspores. The three cells closest to the micropylar end aborted, leaving the functional megaspore (fig. 7*D*) to undergo mitosis and form a two-nucleate megagametophyte with a large vacuole in the center of the cell. This caused the nuclei within the megagametophyte to move to the opposite ends of the cell. The binucleate megagametophyte then underwent two further karyotic divisions to become eight-nucleate (fig. 7*E*). Megametophyte cellularization proceeded to the seven-celled mature megagametophyte. After fertilization the megagametophyte became the embryo sac (fig. 7*F*) and developed into the seed (Kennell and Horner 1985).

The MT female ovule development began similar to that of the WT ovule (fig. 7*G*–7*I*). Meiosis was not observed (fig. 7*I*), even though young megagametophytes were seen to form before they showed signs of collapse and eventual abortion (fig. 7*J*, 7*K*). These ovules continued to develop for a short time (fig. 7*L*) before they aborted and contributed to cessation of pod development, as already shown in figure 2*D*.

SEM

Anthers in both WT and MT flowers showed no outward visible difference (fig. 8*A*, 8*D*). In the WT, the pollen grains were

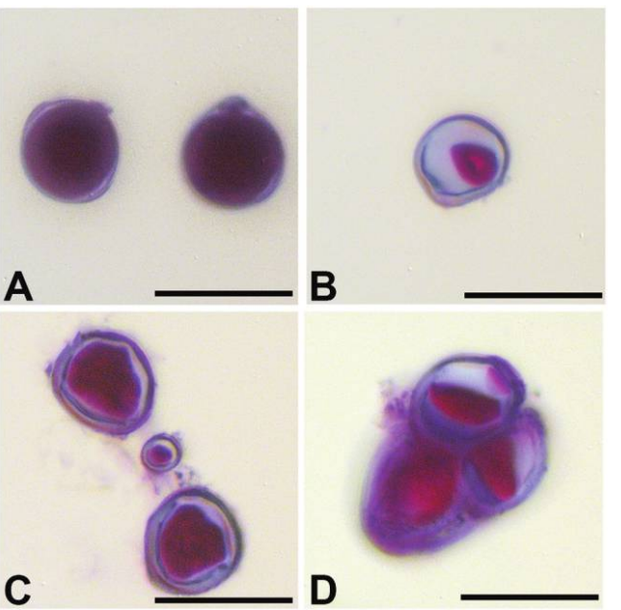

Fig. 4 Alexander staining of pollen taken from mature anthers in wild-type (WT) and mutant (MT) plants. *A*, WT shows complete filling of the pollen grain, indicating viability. *B–D*, Incomplete filling of MT pollen and variable shapes, indicating less viability. Scale bars = 50 μm.

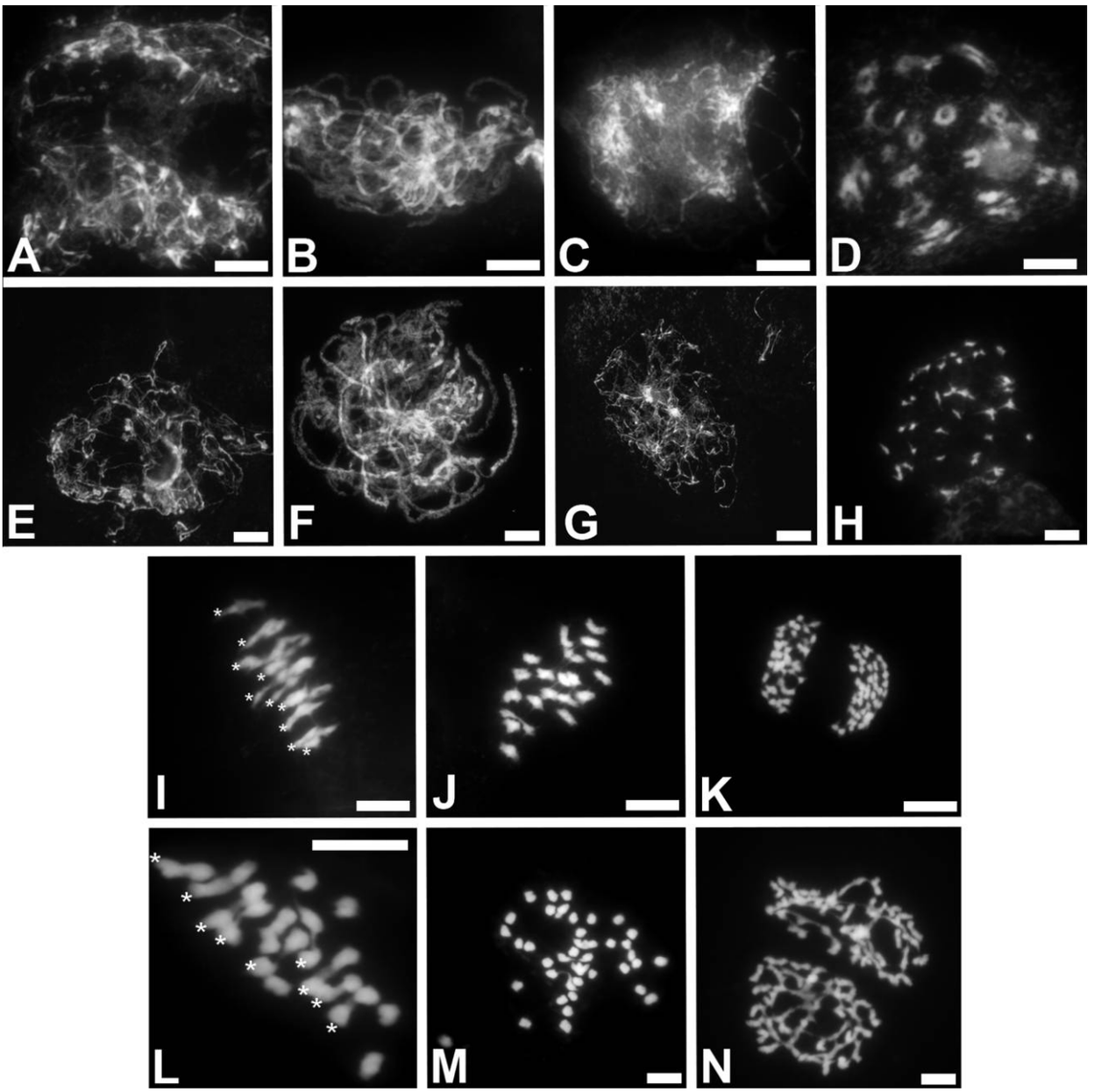

Fig. 5 Chromosome spreads of wild-type (WT) and mutant (MT) male cells at different meiotic stages. Leptotene: *A* (WT), *E* (MT). Pachytene: *B* (WT), *F* (MT). Diplotene: *C* (WT), *G* (MT). Diakinesis: *D* (WT), *H* (MT). Metaphase I: *I* (WT), *L* (MT), *J* (WT), *M* (MT). Anaphase I: *K* (WT), *N* (MT). Asterisks designate bivalents in *I* (WT) and *L* (MT). Scale bars = 20 μm.

uniform in size and tricolporate, and the exine had a normal architecture (fig. 8*G*). Most WT pollen grains were noted with pollen tubes germinating either in the dehiscing anthers or on the WT stigma (fig. 8*B*). The MT male cells (microspores or pollen) were of varying sizes and state of collapse. No pollen tubes were observed, whether in the anthers (fig. 8*F*) or on the MT stigma of the gynoecia (fig. 8*E*), indicating that they were nonviable. The MT pollen exines displayed a variety of patterns, in contrast to the normal WT pollen exines: large pollen showed abnormally formed exines and sometimes collapsed colpi and pores (fig. 8*H*) and frequently collapsed medium-sized pollen (fig. 8*I*), and small pollen showed abnormal shapes and different surface exines (fig. 8*J*).

Discussion

In this study a comprehensive microscopic cytological investigation was done on an MSFS soybean mutant originating from a *w4*-m line that contains the transposon *Tgm9*. In the

w4-m line *Tgm9* was located in the *DFR2* gene that is responsible for anthocyanin pigment in flowers (Xu et al. 2010). With the insertion of *Tgm9* into this locus, white flowers are produced. Since *Tgm9* is a highly active element, excision occurs frequently, restoring the purple color to flowers. When this restored purple flower line progresses to the next generation, the progeny with purple flowers are called germinal revertants. It is from these germinal revertants that the MSFS mutant was identified. According

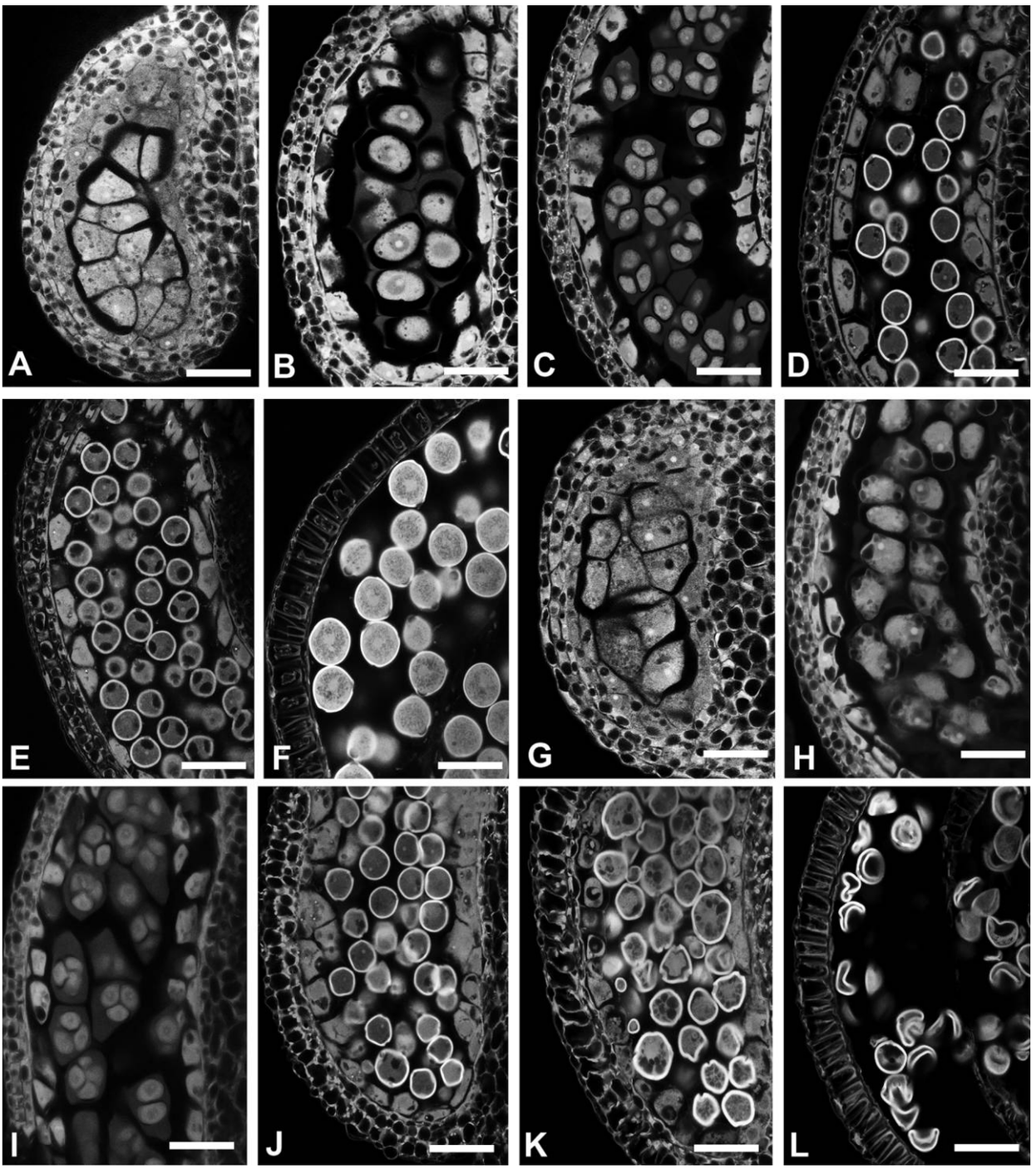

Fig. 6 Confocal scanning laser microscope clearings of soybean wild-type (WT) and mutant (MT) male anthers. *A–F*, WT anther male cell development by stage. *A*, Sporogenous mass. *B*, Meiocytes. *C*, Tetrads. *D*, Early microspores. *E*, Mid- to late-uninucleate microspores. *F*, Binucleate pollen. *G–L*, MT anther male cell development by stage. *G*, Sporogenous mass. *H*, Meiocytes. *I*, Tetrads. *J*, Early microspores. *K*, Mid-microspores. *L*, Aborted late-uninucleate microspores and pollen. Scale bars = 25 μm.

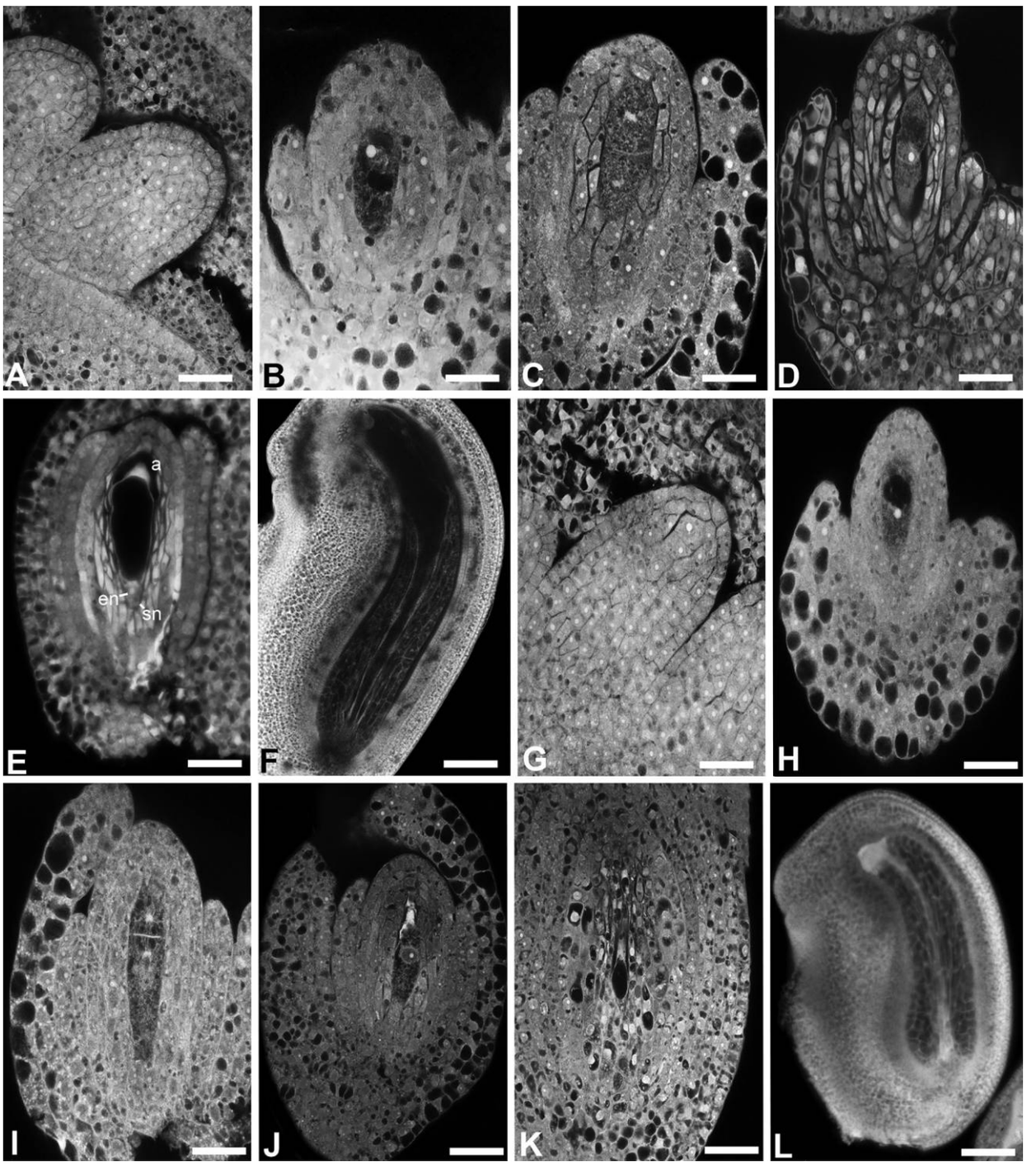

Fig. 7 Confocal scanning laser microscope clearings of soybean wild-type (WT) and mutant (MT) female ovule development. *A–F*, WT ovule development by stage. *A*, Ovule primordium. *B*, Megaspore mother cell. *C*, Dyad. *D*, Functional megaspore. *E*, Eight-nucleate megagametophyte (a = antipodals, en = egg nucleus, sn = synergid nucleus). *F*, Embryo sac. *G–L*, MT ovule development by stage. *G*, Ovule primordium. *H*, Megaspore mother cell. *I*, Dyad. *J*, Functional megaspore and three collapsed micropylar megaspores. *K*, Megagametophyte (partial collapse). *L*, Megagametophyte (complete collapse). Scale bars = 25 μm.

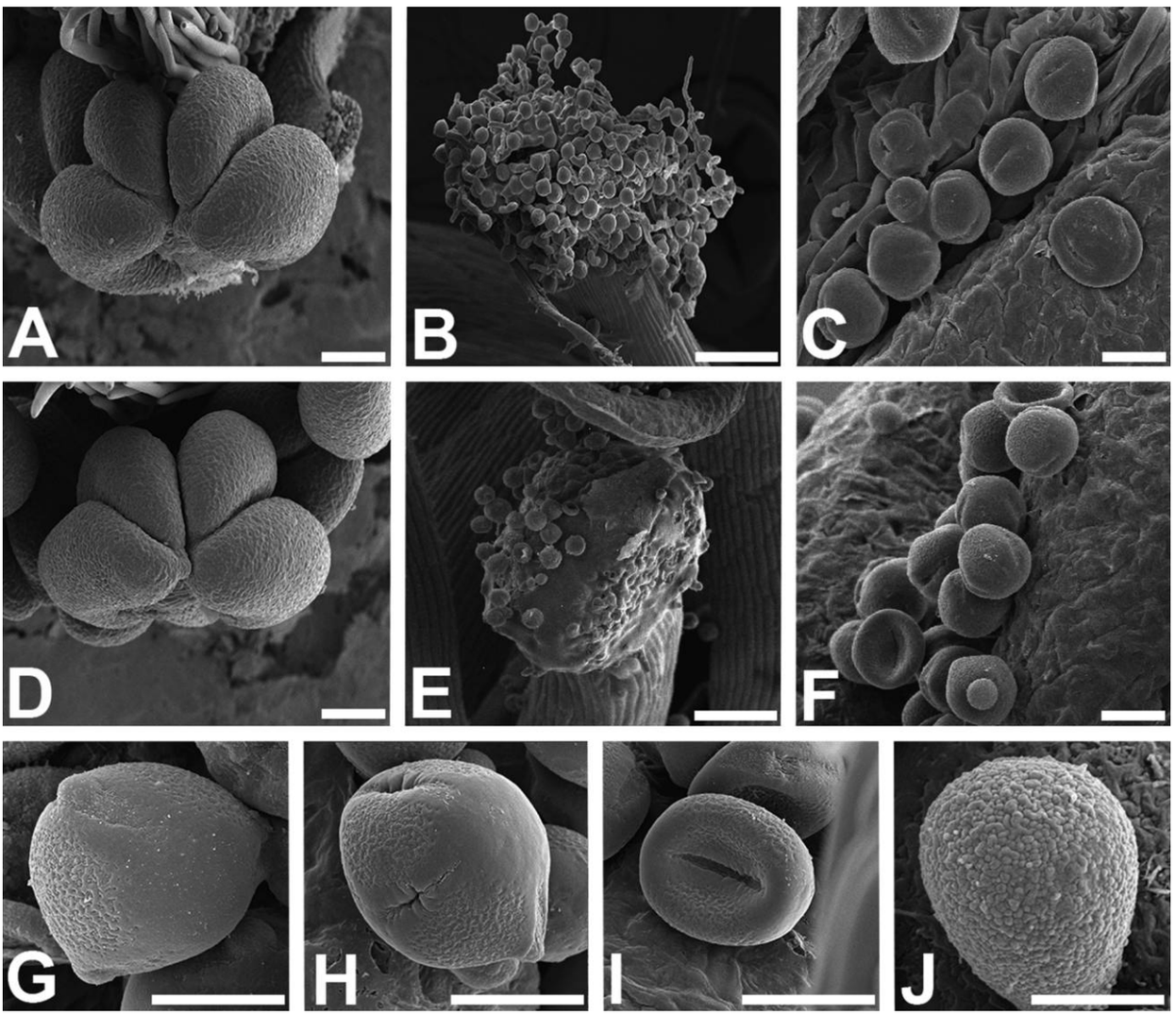

Fig. 8 Scanning electron micrographs of wild-type (WT; *A*–C, *G*) and mutant (MT; *D*–*F*, *H*–*J*) anthers and pollen. *A*, WT anther top view. *B*, WT germinating pollen on stigma. *C*, WT dehisced anther with normal-sized pollen. *D*, MT anther top view. *E*, MT pollen of different sizes on stigma. *F*, MT dehisced anther with collapsed and different-sized pollen grains. *G*, WT tricolporate pollen. *H*, MT large aborted pollen grain. *I*, MT medium collapsed pollen grain. *J*, MT small pollen grain. Scale bars = 100 μm (*A*, *B*, *D*, *E*), 20 μm (*C*, *F*), 10 μm (*G*–*I*), 2 μm (*J*).

to R. G. Palmer (personal communication, April 2014), crosses using WT pollen with the MSFS female plants and MSFS pollen with the WT plants produced no seed. The fertility gene was mapped to the *St8* position on a molecular linkage group J (Raval et al. 2013). This *St8* gene was then cloned using *Tgm9*. One possible candidate, *Glyma.16G072300*, encodes *MER3* that is a DNA helicase gene (Wang et al. 2009). Genetic and molecular work done by Baumbach et al. (2016) showed that the encoded protein has a high similarity to the *Arabidopsis* Rock-N-Rollers (RCK) MER3 DNA helicase. *MER3* is found to be critical in meiotic crossing over, so that mutant *mer3* shows a reduction in bivalent formation during meiotic chromosome pairing in *Arabidopsis* (Mercier et al. 2005). The results of the current study confirm this phenotype as described in other *mer3* mutants (Terasawa et al. 2007).

There were no visible vegetative differences between the growth of the WT and MT plants (fig. 2*A*, 2*B*), indicating that the gene expression occurs in the reproductive tissues. The MT floral development was normal until pod formation, when the WT formed pods that enlarged with developing seed(s) while the MT line formed small sterile pods that never developed further. Of the 84 MT plants that were genotyped, none had any seed set, indicating a true sterile line.

The acetocarmine staining of MT male cells showed abnormalities by the tetrad stage leading to triads, tetrads, pentads, and other various combinations. The Alexander staining for viability of the pollen showed that in the WT all of the 50 pollen grains that were observed showed the dark magenta staining, indicating that the pollen was viable (Peterson et al. 2010). In the MT line, all of the 50 male cells showed magenta staining;

however, the cytoplasms were either plasmolyzed or showed incomplete filling of the cells.

The chromosome spreads during meiosis I helped to confirm the phenotype of *mer3* (Mercier et al. 2005) and showed that meiosis proceeded normally in the MT line until metaphase I, where there was a reduced number of bivalents. In WT there are typically 20 bivalents, while in the MT the number of bivalents ranged from three to nine in total. This significant reduction in bivalents and increased number of univalents created an unbalanced distribution of chromosomes, leading to abnormal tetrad to pollen formation.

The CSLM clearing observations defined which developmental stages proved fatal because of uneven chromosome distribution. On the male side the MT progressed past the tetrad stage but resulted in male cells of varying sizes that became highly vacuolated and eventually collapsed. On the female side, MT development occurred until the megagametophyte stage, where collapse and abortion were evident. This is presumed to be a *mer3*-like effect disrupting meiosis, leading to unbalanced chromosome numbers that result in cell death. This study therefore confirms the presence of the *mer3* gene phenotype for the first time in soybean. It also confirms the use of the *w4*-m line as a useful system to study genes in soybean by identifying new phenotypes as the transposon inserts into other gene loci.

In addition, this study of a meiotic mutant causing MSFS in soy adds to the knowledge base of sterility mutants already existing in soy (Ilarslan et al. 1999). Last, it opens the possibility for continued work that could lead to differential expression of sterility on just the male side in development of a stable hybrid soybean.

Acknowledgments

We dedicate this publication to the memory of Dr. Reid G. Palmer, who laid the foundations for this work. We thank Dr. Madan K. Bhattarchyya and Dr. Silvia R. Cianzio for helpful comments and input on the experiment and manuscript; Jordan Baumbach for her assistance and knowledge on the male-sterile, female-sterile line; Anne Kramer and Taylor Peterson for greenhouse help; and the Iowa State Microscopy and Nanoimaging Facility and staff for equipment use.

Literature Cited

Baumbach J, RN Pudake, C Johnson, K Kleinhans, A Ollhoff, RG Palmer, MK Bhattacharyya, D Sandhu 2016 Transposon tagging of a male-sterility, female-sterility gene, *St8*, revealed that the meiotic MER3 DNA helicase activity is essential for fertility in soybean. PLOS One 11:e0150482.

Bioengineering Confocal and Multiphoton Imaging Core Facility 2000 Clearing Agents. University of Pennsylvania School of Engineering and Applied Science, Philadelphia. http://www.seas.upenn.edu/~confocal/Clearingagents.html#babb.

Ilarslan H, HT Horner, RG Palmer 1999 Genetics and cytology of a new male-sterile, female-sterile soybean mutant. Crop Sci 39:58–64.

Kennell JC, HT Horner 1985 Megasporogenesis and megagametogenesis in soybean, *Glycine max*. Am J Bot 72:1553–1564.

Mercier R, S Jolivet, D Vezon, E Huppe, L Chelysheva, M Giovanni, F Nogué, et al 2005 Two meiotic crossover classes cohabit in *Arabidopsis*: one is dependent on *MER3*, whereas the other one is not. Curr Biol 15:692–701.

Palmer RG, HB Benavente, RW Groose 1989 *w4*-mutable line in soybean. J Genet Dev 10:542–551.

Peterson R, JP Slovin, C Chen 2010 A simplified method for differential staining of aborted and non-aborted pollen grains. Int J Plant Biol 1:e13.

Raval J, J Baumbach, AR Ollhoff, RN Pudake, RG Palmer, MK Bhattacharyya, D Sandhu 2013 A candidate male-fertility female-fertility gene tagged by the soybean endogenous transposon, Tgm9. Funct Integr Genom 13:67–73.

Ross K, P Fransz, G Jones 1996 A light microscopic atlas of meiosis in *Arabidopsis thaliana*. Chromosome Res 4:507–516.

Ruzin SE 1999 Plant microtechnique and microscopy. Oxford University Press, New York.

Terasawa M, H Ogawa, Y Tsukamoto, M Shinohara, K Shirahlge, N Kleckner, T Ogawa 2007 Meiotic recombination-related DNA synthesis and its implication for cross-over and non-cross-over recombinant formation. Proc Natl Acad Sci USA 104:5965–5970.

Wang K, D Tang, M Wang, J Lu, H Yu, J Liu, B Qian, et al 2009 MER3 is required for normal meiotic crossover formation, but not for presynaptic alignment in rice. J Cell Sci 122:2055–2063.

Weigelt HD, RG Palmer, RW Groose 1990 Origin of the *w4-m* allele. Soybean Genet Newsl 17:80–84.

Xu M, HK Brar, S Grosic, RG Palmer, MK Bhattacharyya 2010 Excision of an active CACTA-like transposable element from DFR2 causes variegated flowers in soybean (*Glycine max* [L.] Merr.). Genetics 184:53–63.